

RSC Advances



This is an *Accepted Manuscript*, which has been through the Royal Society of Chemistry peer review process and has been accepted for publication.

Accepted Manuscripts are published online shortly after acceptance, before technical editing, formatting and proof reading. Using this free service, authors can make their results available to the community, in citable form, before we publish the edited article. This *Accepted Manuscript* will be replaced by the edited, formatted and paginated article as soon as this is available.

You can find more information about *Accepted Manuscripts* in the [Information for Authors](#).

Please note that technical editing may introduce minor changes to the text and/or graphics, which may alter content. The journal's standard [Terms & Conditions](#) and the [Ethical guidelines](#) still apply. In no event shall the Royal Society of Chemistry be held responsible for any errors or omissions in this *Accepted Manuscript* or any consequences arising from the use of any information it contains.

Solid polymer substrates and smart fibres for the selective visual detection of TNT both in vapour and in aqueous media

Jesús L. Pablos,* Miriam Trigo-López, Felipe Serna, Félix C. García, José M. García*

Table of contents



Visual detection of the explosive TNT with sensory polymer films and coated fibres

ARTICLE

Solid polymer substrates and smart fibres for the selective visual detection of TNT both in vapour and in aqueous media

Cite this: DOI: 10.1039/x0xx00000x

Received 00th January 2012,
Accepted 00th January 2012

DOI: 10.1039/x0xx00000x

www.rsc.org/

Jesús L. Pablos,* Miriam Trigo-López, Felipe Serna, Félix C. García, José M. García*

This work describes the design of efficient, inexpensive and easily prepared selective sensory polymers with chemically anchored amine groups as 2,4,6-trinitrotoluene (TNT)-sensing motifs as materials for the selective visual detection of TNT in aqueous media and as vapours. The materials are prepared as handleable sensory films or dense membranes from which sensory discs are cut, as well as smart fibres by coating conventional and commercial cotton fabrics. Both types of materials exhibited a highly visible colour development from colourless to red upon contact with TNT both in the gas phase and in solution, and the colour change was used to build titration curves using the colour definition parameters of a digital image acquired with a smartphone, i.e., the RGB system. The materials were selective, remaining silent with other nitroaromatic compounds, such as 4-nitrotoluene and 2,4-dinitrotoluene, and the detection limit in solution was close to the micromolar range.

Introduction

The societal concern about the detection of explosives, related to homeland security, stems mainly from the fear of terrorist attacks. However, their detection and quantification are challenging for forensic and criminal investigations after terrorist acts, for reducing the fatalities that occur during humanitarian efforts in demining, and for health and environmental control and remediation of water and contaminated soils in old military areas and in industrial wastes and spills by explosive-related industries.

Among the various explosives, TNT (2,4,6-trinitrotoluene) belongs to the nitroaromatic explosive family and is one of the most widely used explosives in civil and military applications as well as by terrorists worldwide. As a chemical, TNT can easily enter groundwater supplies and is considered toxic at concentrations above 2 ppb, presenting harmful effects to all biota.¹ For humans, it is a liver toxin that can be absorbed by the gastrointestinal track or even by the skin.²

Accordingly, the detection and quantification of TNT is of the utmost importance and can be performed using a broad set of analytical techniques, such as high performance liquid chromatography (HPLC) and high-resolution gas chromatography (HRGC) paired with different detectors, including mass spectrometry (MS), electrochemical detection (ED), electron capture detectors (ECD), and ultraviolet detectors (UV).¹ However, the use of recognition processes in supramolecular chemistry and novel selective and sensitive optical probes have arisen as promising techniques for the detection of explosives by non-specialised personnel in an *in situ*, rapid and inexpensive manner, both for vapour and in-solution detection; the sensitivity is usually achieved using a quenching strategy based on the use of conjugated polymers or supported solids.³⁻¹⁴

In a recent paper, we demonstrated an insanely simple, novel, and straightforward methodology to prepare handleable solid materials for the naked eye detection of TNT in water environments.¹⁵ Using a commercial monomer containing a tertiary amine, 2-(dimethylamino)ethyl methacrylate (AEMA), we prepared the most inexpensive sensory film that changed its colour upon dipping in aqueous media containing a low concentration of TNT. The sensing mechanisms corresponded to the formation, under mild conditions, of colour complexes of Lewis bases, such as the mentioned amine-containing monomer, with electron-deficient aromatic rings, such as TNT, known since the first decade of the former century as Meisenheimer complexes.¹⁶⁻²⁰

The tuning of the amine motif chemical characteristics of sensory monomers permits not only the lowering of the detection limits in aqueous solutions but also the achievement of TNT vapour detection, an especially cumbersome task due to the extremely low vapour pressure of TNT (9.2 ppb_v).²¹ Thus, the use of both commercial and designed sensory monomers with primary and secondary amines, more active towards the formation of Meisenheimer complexes than tertiary amines, would most likely allow for the two-fold detection and quantification of explosives, i.e., as vapours and in solution. From an applied viewpoint, the former is related to homeland security and humanitarian efforts, and the latter is related to forensic and criminal investigations of washed scrap-metals and residues essential in terrorist-strike investigations and environmental control and remediation.

Thus, we have prepared two film-shaped solid sensory membranes: the first one using the commercial monomer 4- $\{N$ -(2-(methylamino)-ethyl)aminomethyl}styrene (**di-AMS**) with two secondary amine groups and the second one using the monomer with

4-(aminomethyl)styrene (AMS), which have a primary amine that was designed and synthesised by us. The objective was to achieve handleable and tractable materials with the highest sensitivity in the colourimetric detection of TNT. Thus, the materials were cut into manageable sensory discs, and the visual detection of TNT was achieved *in situ* based on clearly visible colour changes of these discs; its quantification was performed using the UV/Vis technique. Moreover, the solid sensory materials also allowed for the direct quantification of the TNT concentration within minutes by processing a digital image taken of these discs using a conventional camera or smartphone using the colour definition, i.e., the RGB parameters, thus avoiding the use of time-consuming techniques operated by skilled and specialised personnel.^{1,22-24} Furthermore, the cotton fibres were coated with the sensory polymers to render wearable TNT sensory intelligent fabrics.

Results and discussion

Strategy followed for the design of the sensory materials

The drive to success in the design of smart materials relies, in our opinion, on the simple idea of selecting a previously described organic, inorganic, or hybrid molecule with a well-known and highly interesting characteristic, functionalising the molecule with the simplest polymerisable chemical group and exploiting the molecule in any environment by copolymerising it with co-monomers that provide the new material with optimal properties, e.g., mechanical and thermal resistance, hydrophilicity or hydrophobicity, or even amphiphilic character.

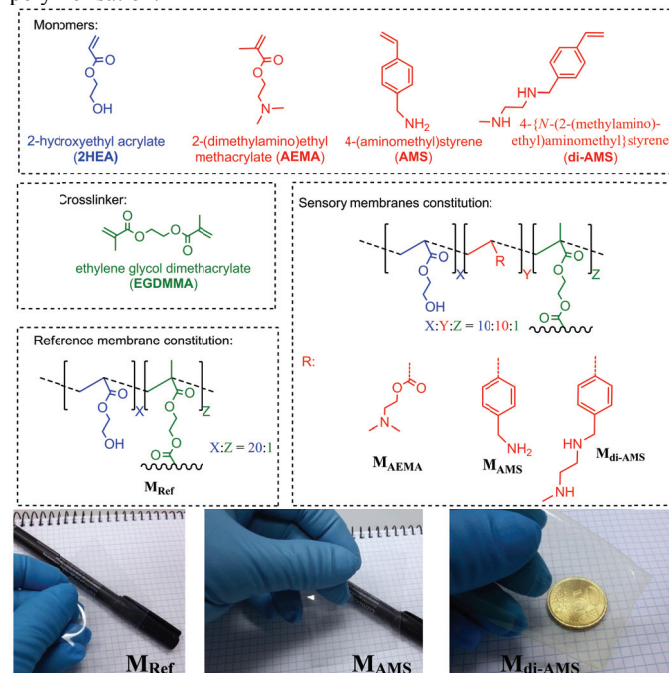
Using this philosophy, numerous chemosensors have been previously described in the literature, most of which are water insoluble organic molecules that work only in organic media. Thus, our objective was to select a well-known chromogenic organic chemosensor, slightly modify its structure by introducing a polymerisable chemical group, and copolymerise it to yield amphiphilic materials that have sufficient hydrophilicity and lipophilicity to be swelled both in water and in organic solvents to allow the target species dissolved in these media to access, by diffusion, the sensory motifs all along the material. In addition, good lipophilicity usually permits the absorption of gases and vapours, thus permitting their detection.

Selecting the colourimetric chemosensory motif for preparing the sensory materials for detecting TNT

As noted in the introduction, Lewis bases, such as amines, alkoxy, and hydroxyl groups form highly coloured Meisenheimer complexes with TNT.¹⁶⁻²⁰ Thus, in a previous paper, we chose a commercial monomer to prepare a chromogenic sensory material for this explosive (AEMA, Scheme 1).¹⁵ This selection was the obvious first choice because the monomer is available commercially and is reasonably priced, and the sensory material was very inexpensive. However, the monomer had a tertiary amine that was the sensory motif, and it is known that a stronger Lewis base character of the amine group leads to a stronger Meisenheimer complex and, concomitantly, greater colour development and sensitivity of the sensory systems. Thus, in a further step, we have prepared sensory materials with secondary and primary amine groups as sensory motifs, and, as expected, the sensitivity towards TNT has been increased without a penalty in selectivity. Moreover, the colourimetric sensory behaviour of the materials has been extended to TNT vapours, whereas the material derived from AEMA, i.e., M_{AEMA} , was insensitive to these vapours.

Preparation and characterisation of the sensory materials

With simplicity in mind and considering our previous work,¹⁵ the planning of naked eye-sensitive sensory materials towards TNT, both in solution and in the vapour phase, involved the design of monomers with secondary and primary amines, as previously mentioned. Accordingly, we found a styrenic commercial monomer with two secondary amines, di-AMS (Scheme 1). Furthermore, using this monomer as a reference, we prepared the simplest styrenic monomer with primary amine groups, AMS. Its synthesis was straightforward and performed in two high-yield conventional synthetic steps, with an overall yield of 84%, starting from the widely used and inexpensive 4-(chloromethyl)styrene (ESI, Scheme S1). A nucleophilic substitution with sodium azide followed by its reduction produced AMS, a monomer that was easily purified by vacuum distillation without adding stabilisers to inhibit premature polymerisation.



Scheme 1. Constitution of the sensory film-shaped dense membranes M_{AMS} and M_{di-AMS} prepared upon the bulk radical copolymerisation of 2HEA and of the sensory monomers AMS or di-AMS, using ethylene glycol dimethacrylate (EGDMA) as the cross-linking agent. The structures of the reference membrane (M_{Ref}), without sensory moieties and of the membrane with tertiary amines as sensory motifs (M_{AEMA}) are also shown.¹⁵ The image of the membranes over a notebook demonstrates the aspect and transparency of the materials.

The constitution of all of the membranes, as derived by FTIR spectra, corresponds to the proposed structure (ν_{OH} , ν_{NH_2} , or ν_{NH} = 3030-3700 cm^{-1} , broad signal; $\nu_{C=O}$ ~ 1722 cm^{-1}), and its spectral pattern resembles the structure of the well-known poly(2-hydroxyethyl methacrylate).²⁵ The spectra of both M_{AMS} and M_{di-AMS} show the characteristic bending of the primary and secondary amine groups as two or one medium to weak intensity bands in the range of 700-850 cm^{-1} and weak bands in the region of 1590-1650 cm^{-1} (Figure S3, ESI).

Thermal resistance is a key parameter of materials for final applications and was evaluated following the weight loss that occurred during the heating of the material at a constant rate (thermogravimetric analysis, TGA). The decomposition

temperatures that resulted in a 5% loss under a nitrogen atmosphere (T_5) were approximately 180 °C, indicating that the materials have a reasonably good thermal stability (Table 1). However, the higher bond energy of the C-O compared with the C-N linkage can be clearly observed in the diminishment of the T_5 at approximately 140 °C of M_{AMS} and M_{di-AMS} compared with M_{Ref} . This negative result is counteracted by the relevant increase of the char yield at 800 °C of M_{AMS} and M_{di-AMS} compared with M_{Ref} due to the partial aromatic structure of the former. The TGA curves are presented in Figure S4, ESI.

Table 1. Thermogravimetric (TGA) analysis (nitrogen atmosphere) and solvent swelling percentage (SSP) data.

Membrane	T_5 (°C)	T_{10} (°C)	T_{ONSET} (°C)	Char yield (%)	SSP (%)	
					water	acetone
M_{Ref}	315	349	286	2	56	40
M_{di-AMS}	171	191	142	14	40	68
M_{AMS}	180	209	165	14	43	53

The amphiphilic character of the materials was related to the water- and acetone-swelling percentage (SSP); that is, the amphiphilic character was related to the weight percentage of solvent uptake by the films upon soaking until equilibrium in pure solvent at 20 °C. This character is key because the membranes must be hydrophilic materials to regain enough water in aqueous media to allow for the chemicals dissolved in water to enter the membrane by diffusion to reach the sensory motifs and to yield the macroscopic signal, indicating the presence of the target molecules. In addition, the lipophilicity of the sensory materials must be sufficient to be solvent-swelled with the same purpose. In our previous experiments, we observed that a SSP between 40% and 100% is optimal for both the rapid diffusion of chemicals into the membrane and for maintaining the tractability, in terms of mechanical properties, of the solvent-swelled materials. All of the sensory membranes meet this criterion, as demonstrated in Table 1. The data clearly indicate a decrement of the hydrophilicity of M_{di-AMS} and M_{AMS} with a parallel increase of the lipophilicity compared with the reference membrane M_{Ref} , with this fact being attributed to the hydrophobic nature of the aromatic ring of the former membranes compared with the latter.

Depicting the interaction of TNT with amines, the sensing phenomenon

It is well established that aromatic nitro-compounds undergo the formation of intensely coloured products with Lewis bases, termed Meisenheimer complexes,¹⁶⁻²⁰ as clearly summarised by Buncl *et al.*, with the complex mechanism concerning the interaction also discussed.²⁶

In our work, the ability of the monomers **AMS** and **di-AMS** to sense TNT in solution was tested before the sensory material preparation. Thus, solutions of the monomers in acetone:water (80:20, v:v) immediately turned reddish after adding TNT, as observed in Figure 1. This aqueous system was selected because of two important application fields related to the use of acetone, with water always present, i.e., the detection of TNT in soils for remediation purposes and for the detection of the explosive used by washing the scrap with acetone after a terrorist attack scenario. The measuring media is important because the water affects the Meisenheimer complex formation by altering the kinetics of these reactions.^{27,28}

The interaction of the monomers **AMS** and **di-AMS** with TNT was confirmed by ¹H NMR. Thus, the addition of TNT to a CDCl₃ solution of the monomers caused the low field shift of the primary

and secondary amine protons, demonstrating the participation of these groups in the Meisenheimer complexes (Figures S5 and S6, ESI). This fact is consistent with the ¹H NMR interaction study of TNT with the monomer **AEMA** with a sensory tertiary amine motif in its structure.¹⁵

The coloured Meisenheimer complexes formed upon interaction in aqueous solution of sensory monomers and TNT in solution permitted the titration of the explosive by UV/Vis, as shown in Figure 2 and Figure S7, ESI. The limit of detection (LOD) and limit of quantification (LOQ)²⁹ of the titration systems were 1×10^{-6} and 3×10^{-6} M, respectively, for the monomers **AMS** and **di-AMS**. Notably, these limits were significantly higher for the monomer with a tertiary amine as the sensory motif, **AEMA** (Table 2), demonstrating the performance increase of the new monomers as sensory probes, as expected.

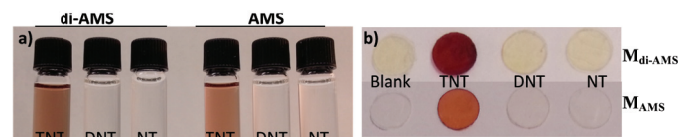


Figure 1. Visual detection of TNT in solution by monomers and sensory membranes: a) images of solutions of **di-AMS** and **AMS** upon addition of TNT, DNT and NT and b) images taken of membranes M_{di-AMS} and M_{AMS} upon dipping in solutions containing TNT, DNT and NT for 10 min. Conditions: solvent acetone:water (80:20, v:v); the concentration of TNT, DNT and NT was $= 1 \times 10^{-2}$ M; in solution experiments [**di-AMS**] and [**AMS**] = 1.2×10^{-3} M.

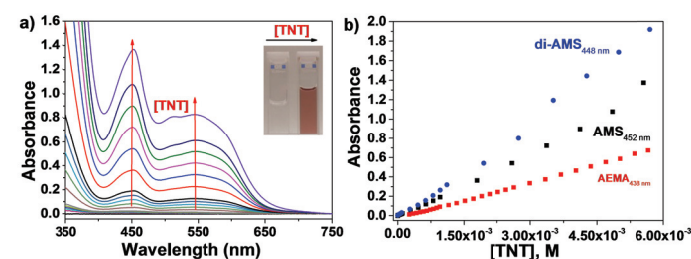


Figure 2. TNT titration by monomers containing amine groups as sensory motifs: a) selected UV/Vis titration curves for monomer **AMS** (inset: image of UV/Vis curves before and after the titration experiments) and b) titration curves for monomers **AMS**, **di-AMS** and **AEMA** (absorbance maxima vs. TNT concentration). Conditions: solvent acetone:water (80:20, v:v); monomer concentration 1.2×10^{-3} M; TNT concentration ranged from 9.9×10^{-8} to 5.5×10^{-3} M.

Table 2. Limit of detection (LOD) and limit of quantification (LOQ) calculated for monomers, membranes and coated fibres.

Monomer	LOD/LOQ $\times 10^6$ M	Membrane	LOD/LOQ Coated fibre	
			$\times 10^5$ M	$\times 10^4$ M
AEMA	19/59	M_{AEMA}	14/43	F_{AEMA} 11/33
di-AMS	1/3	M_{di-AMS}	8/24	F_{di-AMS} 5/16
AMS	1/3	M_{AMS}	9/26	F_{AMS} 4/11

Sensory membranes for the detection of TNT in solution

Visual preliminary studies with the dense membranes M_{di-AMS} and M_{AMS} revealed an effective colour development upon dipping in solutions containing TNT for only 10 min, thus indicating a rapid

and efficient formation of the Meisenheimer complex (Figure 1). However, the reference material, M_{Ref} , produced no colour change, as expected. The colour changes were apparent within the first minute.

The response time of the materials was evaluated by UV/Vis spectroscopy. Sensory discs of M_{di-AMS} and M_{AMS} were immersed in a quartz cuvette containing acetone:water (80:20, v:v), and the UV/Vis spectra were recorded. Then, TNT was added to the cuvette from a concentrated stock acetone:water (80:20, v:v) solution, and UV/Vis spectra were recorded as a function of time (Figure S8, ESI). While the absorption maxima due to colour development were noted immediately after the addition of TNT, in our opinion, a better measuring time using the UV/Vis technique would be 20 min because the absorbance maxima is approximately 1. However, for visual and photographic analysis, a dipping time of 1 hour was considered because the colours were more intense and higher sensitivity was envisaged, and longer times were not deemed useful due to the instability of the Meisenheimer complexes under ambient conditions and the decomposition of TNT in solution.

The visual sensing performance of the sensory membranes involved analysing immersed discs of M_{di-AMS} and M_{AMS} in solutions of various concentrations of TNT for 1 hour, rendering discs of different colour intensities, as depicted in Figure 3. A visible colour change was observed at a TNT concentration of 1×10^{-4} M. After the colour change, digital images of the discs were taken, and the colour definition of each disc was related to the TNT concentration to build the titration curve. As the colour is defined in the RGB system by the three variables red (R), green (G) and blue (B), ranging from 0 to 255, the information regarding these variables were joined in a single result (principal component 1, CP1) using principal components analysis (PCA), accounting for >92% of the information on the three RGB parameters. Using a straightforward mathematical workup, this strategy permits the use of nearly all of the colour information to prepare simple [TNT] vs. CP1 titration curves (the principal component parameters and RGB data are listed in Tables S2–S9, ESI).

The sensitivity was within the millimolar and micromolar range, improving the performance of the previously described sensory membrane M_{AEMA} (Table 2). Regarding the selectivity, neither the monomers in solution nor the sensory membranes changed their colour with other nitro-aromatics besides TNT and especially remained silent with the related NT and DNT, as visually observed in Figure 1.

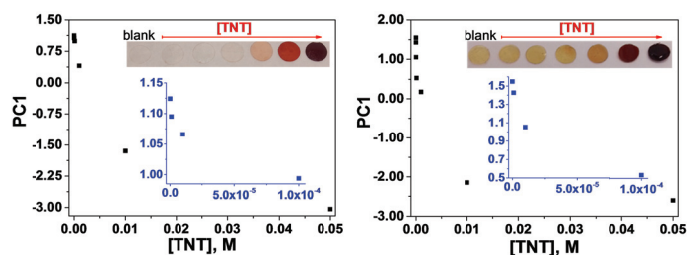


Figure 3. Titration of TNT with sensory discs of membranes M_{AMS} (left) and M_{di-AMS} (right) using the RGB parameters from digital images taken of the sensory materials. The images were taken after immersing the discs in acetone:water (80:20, v:v) solution for 1 h, and three parameters (R, G and B) defining the colour of each disc were reduced to one principal component (PC1) by principal component analysis. The images of the discs depict the colour variations arising from the differences in the concentration of TNT (Blank, 1×10^{-6} , 1×10^{-5} , 1×10^{-4} , 1×10^{-3} , 1×10^{-2} , 5×10^{-2} M).

Smart fibres for the detection of TNT in solution

Smart or intelligent textiles are stand-alone systems that can be used as sensors, actuators, communication devices, energy sources and storage tools, and even processors and a new generation of textiles made of stimuli-responsive fibres are expected in the near future to contribute significantly to our health and safety.³⁰⁻³²

Within this context, intelligent fabrics capable of detecting TNT represent an attractive class of substrates for fabricating wearable chemical polymeric sensors.³³ Accordingly, we describe herein the coating of cotton fibres of white fabric pieces cut from a lab coat as smart textiles for the colourimetric sensing of TNT. Squares of 1×1 cm of the lab coat were coated with sensory polymers prepared from sensing co-monomers AMS and $di-AMS$, fabrics F_{AMS} and F_{di-AMS} , respectively, as well as $2HEA$, $EGDMA$ and a radical photoinitiator. Thus, following the same behaviour as the sensory membrane discs described in the previous section, the smart textiles turned reddish upon interaction with TNT in solution, as observed in Figure 4. Noticeably, the detection time was very short, and the colour change was complete in 5 min, which was significantly less time than that required for the sensory membranes, most likely due to the rapid access of the TNT to the sensory motifs of the thin coating compared with the time needed to diffuse inside the solvent-swelled dense membrane.

Following the same procedure used for the sensory membranes, digital images of the sensory fabric dipped in acetone containing various concentrations of TNT permitted the construction of titration curves (Figure 4) with LOD and LOQ within the micromolar range (Table 2), and this LOD was also clearly visually observed.

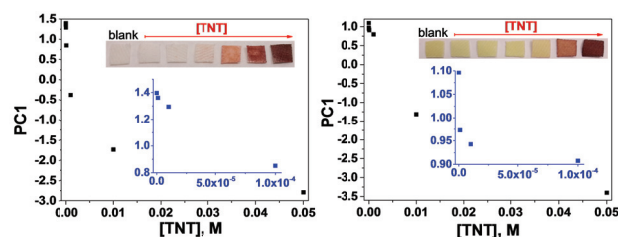


Figure 4. Titration of TNT with cotton coated fibres F_{AMS} (left) and F_{di-AMS} (right) using the RGB parameters from digital images taken of the sensory materials. The images were taken after immersing the lab coat square fabrics in acetone:water (80:20, v:v) solution for 5 min, and three parameters (R, G and B) defining the colour of each square were reduced to one principal component (PC1) using principal component analysis. The images of the squares depict the colour variations arising from the differences in the concentration of TNT (Blank, 1×10^{-6} , 1×10^{-5} , 1×10^{-4} , 1×10^{-3} , 1×10^{-2} , 5×10^{-2} M).

Sensory membranes for the detection of TNT vapours

The detection of nitroexplosive vapours is especially important for many applications related to explosive sensing, for instance in civil security or weapon elimination. However, their detection is cumbersome due to their extremely low vapour pressures, particularly with chromogenic chemical sensing, where a visual signal arises from the feeble interaction or from the reaction of the explosive molecules with a receptor.

Thus, a slight colour change is observed at room temperature for the dense membrane M_{di-AMS} and M_{AMS} upon sealing cut sensory discs in small vials containing small quantities of TNT. Noticeably, this behaviour was not observed for the materials with tertiary amines as sensory groups, M_{AEMA} .

Based on this observation, the sensory performance of sensory discs cut from M_{di-AMS} and M_{AMS} was analysed. To increase the

colourimetric response and to expedite the experimental workup, the experiments were performed at 60 °C, where the vapour pressure of TNT is two orders of magnitude higher than at 25 °C, i.e., 829 ppb_v, according to the equation $\text{Log } P (\text{ppb}_v) = (-5481/T) + 19.37$, where T is the temperature in K.³⁴ The colour development was similar to that observed in the detection of TNT in solution and was clearly observed by the naked eye and followed by UV/Vis spectroscopy, as depicted in Figure 5 and in Figure S9, ESI. As expected, no change was observed for the reference material M_{Ref} .

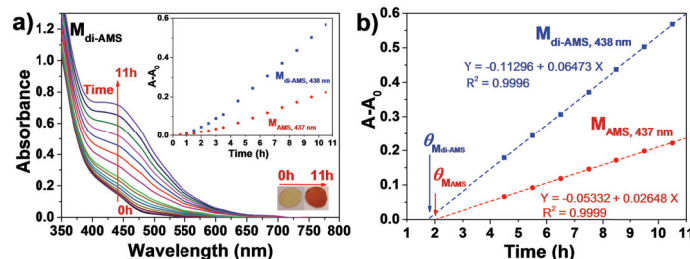


Figure 5. Detection of TNT with sensory membranes M_{AMS} and $M_{\text{di-AMS}}$ using a UV/Vis technique as a function of time: a) UV/Vis spectra of membrane $M_{\text{di-AMS}}$ in an atmosphere containing TNT vapours (insets: image of the sensory discs and relative absorbance vs. time of membranes M_{AMS} and $M_{\text{di-AMS}}$); b) linear region (steady state) of absorbance increase vs. time of membranes M_{AMS} and $M_{\text{di-AMS}}$, showing the time intercept of the linear regression curve (time lag, θ). Experimental conditions: 50 mg of TNT in a conventional sealed measuring quartz cuvette; temperature: 60 °C.

The vapour sensing phenomena occur due to a diffusion/interaction mechanism, i.e., the vapour enters the membrane by diffusion, and in parallel, the interaction to render the Meisenheimer complexes takes place. The behaviour of the system in terms of diffusion clearly resembles that of gas transport through membranes, where the steady state is characterised by a straight line in pressure vs. time curves and is achieved after a time lag (ϕ) calculated at the intersection of the straight line fit corresponding to the straight line region with the abscissa.^{35,36} Thus, the flux of TNT molecules inside the membrane keeps the concentration of TNT in the centre of the membrane near zero because the molecules react with amine groups to yield the coloured complexes. The TNT gradient across the membrane is maintained until all of the amine groups interact with TNT, achieving a steady state at a certain time, and this state is maintained at least throughout the experiment, i.e., 11 h. The time lag is similar for both membranes (Figure 5) and can be related to the diffusion coefficient (D) for Fickian diffusion, with both the solubility coefficient and D independent of concentration, by $D = l^2/6\phi$, where l is the thickness of the membranes in gas transport experiments, where the pressure on one side of the membrane is negligible. In our systems, as the membrane is in a TNT vapour atmosphere, the concentration gradient is from both sides of the membrane to the centre, where the zero concentration of unreacted TNT could be considered, and l would be half of the experimental membrane thickness.³⁵ Thus, ϕ is 1.75 and 2.01 h for $M_{\text{di-AMS}}$ and M_{AMS} , respectively, and D is 8.3×10^{-10} and 8.0×10^{-10} cm²/s. The higher slope of the relative absorbance increase vs. time, visually observed by a deeper colour development, for $M_{\text{di-AMS}}$ compared with M_{AMS} may arise from the fact that each di-AMS monomer has two amine groups, while AMS only has one, and the real sensory motif density arising from the same molar feed ratio in each membrane is twice as large in $M_{\text{di-AMS}}$ compared with M_{AMS} . In addition, the lone pair of the secondary amine is more external than

that in the primary amine, giving the former a higher nucleophilic character.

The need to raise the temperature of the experiments to increase the TNT vapour concentration is a clear disadvantage for any practical application, where the explosive must be detected at ambient temperature. However, by working with membranes and smart fabrics that can transport gases by applying a pressure gradient, it is envisaged that a system could be designed to force air by pressure or vacuum on one side of the materials to concentrate the explosive vapours inside the membrane or coating, where the molecules would rapidly undergo the Meisenheimer complex formation.

Smart fibres for the detection of TNT vapours

In a similar fashion, the smart fabrics F_{AMS} and $F_{\text{di-AMS}}$ change their colour from white to red upon contact with TNT vapours. The experiments were performed qualitatively at 60 °C, and the slight reddish colour observed in the first two hours of exposure turned deep red in 11 h, as observed in Figure 6.



Figure 6. Visual detection of TNT vapours with coated fibres. Conditions: approximately 0.4 x 0.8 cm of each fabric was suspended in a sealed vial with 50 mg of TNT at 60 °C for 11 h.

Conclusions

In this study, we demonstrate the potential of polymers in cutting edge technological applications such as the naked eye detection of explosives following a chemosensory approach. The design of solid sensory polymeric substrates with chemically anchored amine groups as TNT-sensing motifs has been undertaken following a simple, straightforward and inexpensive approach to render usable films or membranes along with coated cotton fibres as smart fabrics for the visual sensitive and selective sensing of TNT both in solution and as a vapour. The visual change of the materials from colourless or white (fibres) to red allowed for the naked eye detection of the explosive, and digital photographs taken of the materials permitted quantification by building titration curves using the colour digital definition, i.e., the RGB parameters, of the materials after being in contact with various concentrations of TNT. Although the detection of TNT vapour is cumbersome, due to its low vapour pressure, we envisage that air forced to permeate through the membranes or fibres could serve as a future system to concentrate the TNT molecules inside of the materials, where the interaction with the sensing motif causes the colour changes, possibly opening the systems to forthcoming security applications.

Acknowledgements

We gratefully acknowledge the financial support provided by the Spanish Ministerio de Economía y Competitividad-Feder (MAT2011-22544) and by the Consejería de Educación-Junta de Castilla y León (BU232U13).

Notes and references

Departamento de Química, Facultad de Ciencias, Universidad de Burgos, Plaza de Misael Bañuelos s/n, 09001 Burgos, Spain. Emails: jlpablos@ubu.es (J.L. Pablos), jmiguel@ubu.es (JM García); Tel: +34 947 258 085; Fax: +34 947 258 831.

ARTICLE

† Footnotes should appear here. These might include comments relevant to but not central to the matter under discussion, limited experimental and spectral data, and crystallographic data.

Electronic Supplementary Information (ESI) available: monomer synthesis and characterisation, sensory membrane preparation and characterisation, fibre coating procedure, measuring conditions, TNT titration data, principal component analysis data. See DOI: 10.1039/b000000x/

- 1 United States Environmental Protection Agency (EPA), Technical Fact Sheet – 2,4,6-Trinitrotoluene (TNT), May 2012 (http://www.epa.gov/fedfac/pdf/technical_fact_sheet_tnt.pdf). Access data: Feb 27, 2014.
- 2 W. D. McNally, Toxicology, Industrial medicine Publishing Co.: Chicago, 1937.
- 3 S. Singh, *J. Hazard. Mater.*, 2007, **144**, 15.
- 4 S. Rochat and T. M. Swager, *ACS Appl. Mater. Interfaces*, 2013, **5**, 4488.
- 5 A. Alvarez, A. Salinas-Castillo, J. M. Costa-Fernández, R. Pereiro and A. Sanz-Medel, *Trac-Trend. Anal. Chem.*, 2011, **9**, 1513.
- 6 S. W. Thomas, G. D. Joly and T. M. Swager, *Chem. Rev.*, 2007, **107**, 1339.
- 7 J. M. García, F. C. García, F. Serna and J. L. de la Peña, *Polym. Rev.*, 2011, **51**, 341.
- 8 S. Content, W. C. Trogler and M. J. Sailor, *Chem. Eur. J.*, 2000, **6**, 2205.
- 9 K. S. Bejoymohandas, T. M. George, S. Bhattacharya, S. Natarajanb and M. L. P. Reddy, *J. Mater. Chem. C*, 2014, **2**, 515.
- 10 J. L. Novotney and W. R. Dichtel, *ACS Macro Lett.*, 2013, **2**, 423.
- 11 A. D. Aguilar, E. S. Forzani, M. Leright, F. Tsow, A. Cagan, R. A. Iglesias, L. A. Nagahara, I. Amlani, R. Tsui and N. J. Tao, *ACS Nano Lett.*, 2010, **10**, 380.
- 12 N. R. Walker, M. J. Linman, M. M. Timmers, S. L. Dean, C. M. Burkett, J. A. Lloyd, J. D. Keelor, B. M. Baughman and P. L. Edmiston, *Anal. Chim. Acta*, 2007, **593**, 82.
- 13 S. Tao, G. Li and J. Yina, *J. Mater. Chem.*, 2007, **17**, 2730.
- 14 S. Tao, G. Li and H. Zhub, *J. Mater. Chem.*, 2006, **16**, 4521-4528
- 15 J. L. Pablos, M. Trigo-Lopez, F. Serna, F. C. Garcia and J. M. Garcia, *Chem. Commun.*, 2014, **50**, 2484.
- 16 J. Meisenheimer, *Justus Liebigs Ann. Chem.*, 1902, **323**, 205.
- 17 F. Terrier, *Chem. Rev.*, 1982, **82**, 77.
- 18 H. Chen, H.W. Chen and G. Cooks, *J. Am. Soc. Mass Spectrom.*, 2004, **15**, 998.
- 19 Y. Liu, H.H. Wang, J. E. Indacochea and M. L. Wang, *Sens. Actuators B*, 2011, **160**, 1149.
- 20 E. Ercag, A. Uzer and R. Apak, *Talanta*, 2009, **78**, 772.
- 21 R. G. Ewing, M. J. Waltman, D. A. Atkinson, J. W. Grate and P. J. Hotchkiss, *TrAC-Trend. Anal. Chem.*, 2013, **42**, 35.
- 22 K. L. Diehl and E. V. Anslyn, *Chem. Soc. Rev.*, 2013, **42**, 8596.
- 23 D. S. Moore, *Rev. Sci. Instrum.*, 2004, **75**, 2499.
- 24 J. Cho, R. Anandakathir, A. Kumar, J. Kumar and P. U. Kurup, *Sens. Actuators B*, 2011, **160**, 1237.
- 25 S. N. Dobić, J. M. Filipović and S. L. Tomić, *Chem. Eng. J.*, 2012, **179**, 372.
- 26 E. Buncel, A.R. Norris and K.E. Rusell, *Q. Rev. Chem. Soc.*, 1968, **22**, 123.
- 27 E. Ercag, A. Uzer and R. Apak, *Talanta*, 2009, **78**, 772-780.
- 28 T.F. Jenkins and M.E. Walsh, *Talanta*, 1992, **39**, 419.
- 29 The limit of detection (LOD) and the limit of quantification (LOQ) were estimated by the following equation: $LOD = 3.3 \times SD/s$ and $LOQ = 10 \times SD/s$, where SD is the standard deviation of a blank sample and s is the slope of the calibration curve in a region of low TNT content.
- 30 L. Van Langenhove, C. Hertleer and A. Schwarz, Smart Textiles: An Overview, in Intelligent Textiles and Clothing for Ballistic and NBC Protection, NATO Science for Peace and Security Series B: Physics and Biophysics, P. Kiekens and S. Jayaraman (eds.), Springer: Dordrecht, 2012, Ch 6, pp 119-136.
- 31 P. Westbroek, G. Priniotakis, P. Kiekens, Intelligent/smart materials and textiles: an overview, in Analytical electrochemistry in textiles, Woodhead Publishing Limited and CRC Press LLC: Cambridge: 2005, Ch 8, pp 215-243.
- 32 K. Cherenack and L. van Pieterse, *J. Appl. Phys.*, 112, 091301.
- 33 M.C. Chuang, J.R. Windmiller, P. Santhosh, G. V. Ramrez, M. Galik, T.Y. Chou and J. Wang, *Electroanalysis*, 2010, **21**, 2511.
- 34 B. C. Dionne, D. P. Rounbehler, E. K. Achter, J. R. Hobbs and D. H. Fine, *J. Energ. Mater.*, 1986, **4**, 447.
- 35 R. M. Felder, G. S. Huvard, Permeation, diffusion, and sorption of gases and vapors, in Polymers, Physical Properties, Methods of Experimental Physics, Vol. 16, Part C, Academic Press: New York, 1980, Ch. 17.
- 36 S. Matteucci, Y. Yampolskii, B. D. Freeman, and I. Pinnau, Transport of Gases and Vapors in Glassy and Rubbery Polymers, in Material Science of Membranes for Gas and Vapor Separation, Y. Yampolskii, B. D. Freeman, and I. Pinnau Eds., Wiley, Chichester: 2006, Ch. 1, pp. 1-47.